

ENABLING AGENTS TO COMMUNICATE ENTIRELY IN LATENT SPACE

Zhuoyun Du^{1†*} Runze Wang^{2†} Huiyu Bai³ Zouying Cao⁴ Xiaoyong Zhu²
 Bo Zheng² Wei Chen¹ Haochao Ying^{1✉}

¹Zhejiang University ²Taobao & Tmail Group of Alibaba

³Nanyang Technological University ⁴Shanghai Jiao Tong University

{duzy, haochaoying}@zju.edu.cn, yunze.wrz@alibaba-inc.com

ABSTRACT

While natural language is the de facto communication medium for LLM-based agents, it presents a fundamental constraint. The process of downsampling rich, internal latent states into discrete tokens inherently limits the depth and nuance of information that can be transmitted, thereby hindering collaborative problem-solving. Inspired by human “mind-reading”, we propose Interlat (Inter-agent Latent Space Communication), a paradigm that leverages the last hidden states of an LLM as a representation of its mind for direct transmission (termed “latent communication”). An additional compression process further compresses latent communication via entirely latent space reasoning. Experiments demonstrate that Interlat outperforms both fine-tuned chain-of-thought (CoT) prompting and single-agent baselines, promoting more exploratory behavior and enabling genuine utilization of latent information. Further compression not only substantially accelerates inference but also maintains competitive performance through an efficient information-preserving mechanism. We position this work as a feasibility study of entirely latent space inter-agent communication, and our results highlight its potential, offering valuable insights for future research.

“We do not have organs of communication. Our brains can display our thoughts to the outside world, thereby achieving communication.”
 — Cixin Liu, *The Dark Forest*.

1 INTRODUCTION

Large language model (LLM)-based agentic systems represent a promising and considerably attractive area of contemporary research (Wang et al., 2025; 2024). This interest stems from their ability to orchestrate detailed workflows through natural language that enable agents to interact and collaborate for complex task solving (Qian et al., 2024; Zhang et al., 2024b; Tran et al., 2025). However, although readable by human, natural language introduces constraints on a model’s expressive range and can also impose redundant computation: LLMs must down-sample their rich, high-dimensional internal states into discrete tokens, typically exposing only a single linear thought in their message, *i.e.*, a chain of thought (CoT) (Wei et al., 2022) plan to advise another agent (Yu et al., 2024). Furthermore, a large portion of the generated text serves to maintain linguistic coherence rather than to convey essential information (Zhang et al., 2024a). This inefficient paradigm results in ambiguous, lossy inter-agent communication that prevents effective coordination (Chen et al., 2025), which remains a primary cause of task failures in multi-agent systems (Cemri et al., 2025).

Human communication, by contrast, is not limited to explicit language; much of it is implicit and nonverbal latent communication (Aviezer et al., 2012; Kelly et al., 2010). This capacity is closely tied to humans’ ability for “mind-reading”, constructing internal models of others to infer latent

[†]Equal Contribution.

*Work done during an internship at Alibaba Group.

✉Corresponding Authors.

intentions (Fletcher et al., 1995; Vogeley et al., 2001). In multi-agent settings, we propose that latent communication provides an analogous form of human mind-reading: instead of inferring others’ thoughts from words, agents transmit representations that can display their latent thoughts for downstream use, enabling tighter alignment of intentions. While direct sharing is technically and ethically challenging for humans, LLM-based agents spend most of their processing budget in the latent space and naturally produce hidden states throughout their intermediate layers, which can be extracted to support direct, expressive communication. Previous works have attempted to use hidden states for communication; however, these approaches either rely on a one-shot activation graft that struggles to carry multiple mind paths. (Ramesh & Li, 2025) or remain constrained by language space, in which hidden states must pair to an already-sampled text trajectory (Tang et al., 2025). Meanwhile, these methods require ad-hoc layer choices, which introduces an extra tuning process.

In this work, we propose Interlat, a novel paradigm for direct inter-agent communication entirely in latent space. Rather than transmitting tokens decoded via the language-model head and embedding layer, Interlat transmits the collected last-layer hidden states for all generated tokens, which we term latent communications, as representations of one agent’s latent thoughts for another agent. Formally, we frame the agent’s mind-reading ability as the ability to differentiate and effectively utilize the rich information contained in the latent communication for the task they are solving. Motivated by the high information density inherent in latent states, inspired by (Hao et al., 2024; Shen et al., 2025; Cheng & Van Durme, 2024), we further train the agent to generate messages in an unconstrained latent space. By learning to generate more information-rich latent states, we successfully compress latent communications into much shorter sequences. This compression yields substantial efficiency improvement while preserving the information needed for downstream tasks.

Experimentally, we focus on a two-agent sender-receiver scenario, which is the fundamental building block of various multi-agent systems, and intentionally avoid orthogonal components such as retrieval, tool use, or multi-round debate orchestration, so as to reduce confounding factors. We evaluate our approach on ALFWorld (Shridhar et al., 2020), a multi-step benchmark requiring planning and execution coordination. Compared to conventional natural language baselines, Interlat achieves performance improvements on both seen and unseen tasks. Analysis reveals that agents utilizing latent communication exhibit more exploratory behavior patterns that lead to higher overall success rates with a genuine understanding of task-relevant latent information rather than superficial pattern matching. Moreover, we demonstrate that latent messages can be compressed to as few as 8 tokens while maintaining competitive performance, achieving up to a 24× reduction in communication latency. Further analysis of the output probability distribution after compression reveals how task-critical information is effectively preserved.

2 RELATED WORK

Latent Reasoning in LLMs. A growing line of work shifts reasoning from the language space to the latent space, replacing explicit CoT traces with multi-step computation in continuous representations to bypass the bandwidth and efficiency constraints of text (≈ 15 bits/token vs. $\approx 40k$ bits/hidden-state) (Zhu et al., 2025b). To increase available compute at inference time, (Goyal et al., 2023) introduces learnable pause tokens that delay the generation of the final answer, while (Pfau et al., 2024) employs filler tokens to scaffold intermediate computations that would be infeasible without generating tokens. Beyond token scheduling, (Liu et al., 2024) proposes a latent coprocessor operating directly on the transformer KV cache to improve performance. Another line of work (Hao et al., 2024; Shen et al., 2025; Cheng & Van Durme, 2024) enables the model to reason in latent space by feeding the last hidden state back as the next input embedding, enabling the model to explore multiple reasoning paths in parallel, akin to a breadth-first search. (Bae et al., 2024; Gao et al., 2024; Geiping et al., 2025) decouple input encoding, iterative reasoning, and output decoding, making the computation more modular and interpretable. Building upon these advantages of latent space for reasoning, our work shifts focus from single-model latent reasoning to enabling inter-agent communication and task solving in latent space.

Multi-agent Communication. LLM-based agent systems typically orchestrate in natural language (Qian et al., 2024; Zhu et al., 2025a; Wang et al., 2024). Although readable by humans, natural language introduces constraints on a model’s expressive range and can also impose redundant computation. (Pham et al., 2023) replaces sampled tokens with probability-weighted tokenizer embeddings,

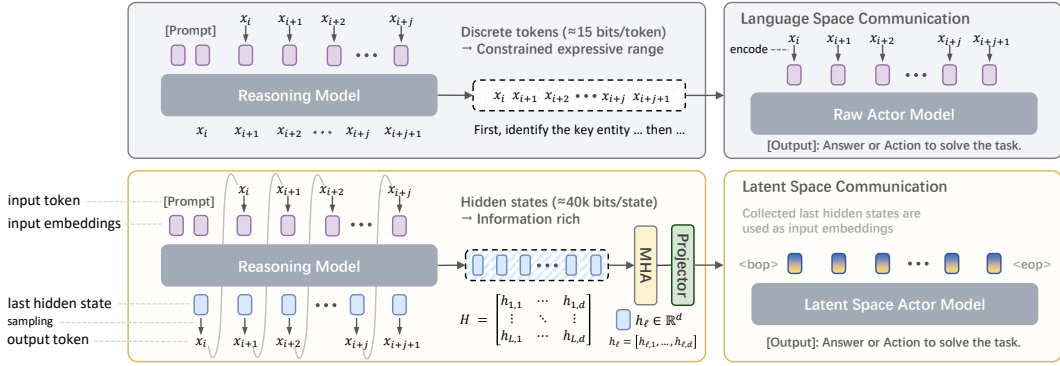


Figure 1: A comparison of Interlat with conventional language-space communication. In language space, an agent transmits a discrete token sequence $[x_i, x_{i+1}, \dots, x_{i+j+1}]$ (e.g., a CoT plan) to another. In Interlat, the model leverages its last hidden states as a representation of its internal “mind” state, processed by a communication adapter, and then transmits them directly to the other agent, enabling communication entirely in latent space with higher expressive capacity.

preserving more of the model’s belief distribution and improving debate performance, but it still communicates surface-level final-layer distributions, overlooking deeper, more informative, and more valuable hidden representations. (Ramesh & Li, 2025) blends hidden states between agents, yielding accuracy gains with less compute than natural-language messages; however, it operates as a single hidden state graft within a pass rather than a temporally structured latent sequence. (Tang et al., 2025) preserves richer information by recording per-token state deltas at selected layers on the sender and adding them at the corresponding layer positions on the receiver while transmitting text, but requires model-specific layer selection and language space text. Building on these valuable insights, we transmit a sequence of last hidden states directly between agents and apply a compression process to enable information-rich, language-free, and efficient communication.

3 INTERLAT

In this section, we formalize how to extract an agent’s states as the representation of its “mind” for inter-agent latent space communication. Let $x = (x_1, \dots, x_T)$ with a prompt $x_{1:m}$ and a completion $y = (y_1, \dots, y_L)$ such that $y_\ell = x_{m+\ell}$ and $L = T - m$. For each decoding step $\ell = 1, \dots, L$, define

$$\begin{aligned} h_\ell &= \text{Transformer}(x_{\leq m+\ell-1})[m + \ell - 1], \\ H &= [h_1, h_2, \dots, h_L], \end{aligned} \quad (1)$$

where $h_\ell \in \mathbb{R}^d$ is the last hidden state immediately before predicting y_ℓ (i.e., at position $m + \ell - 1$ in the full sequence). $H \in \mathbb{R}^{L \times d}$ collects these last-layer hidden states for the completion region.

3.1 LATENT COMMUNICATION

Our Interlat removes natural language constraints by letting agents transmit their thoughts by directly passing the collected last hidden states, which we termed **latent communication**. As shown in Figure 1, this transmission occurs at the end of an agent’s message generation process. Special tokens, $x_i = \langle \text{bop} \rangle$ and $x_j = \langle \text{eop} \rangle$, are added to mark the beginning and the end of the latent communications. Consider an agent \mathcal{M}_i solving a task $\mathcal{T} = \{x_1, \dots, x_m\}$. Upon receiving a latent communication $H = \{h_1, h_2, \dots, h_L\}$ from another agent, \mathcal{M}_i forms its input embedding sequence as:

$$E = [e(x_1), e(x_2), \dots, e(x_i), h_1, h_2, \dots, h_L, e(x_j)],$$

where $e(\cdot)$ is the token embedding function. This inference process is analogous to standard language space multi-agent systems, except that it feeds hidden states between agents. The latent communications have been processed by a trainable light-weight self-attention and a projection layer as a communication adapter for magnitude rescaling and helping the agent better interpret the latent meaning within these latent representations. For brevity, we may refer to latent communications as *latents* where unambiguous.

3.2 TRAINING PROCEDURE

In this work, we consider two agents: a *reasoning* agent as a sender that produces a task-specific plan together with its final-layer latent states, and an *actor* agent as a receiver that consumes this information to generate actions to solve tasks, which is the basic unit for sophisticated systems.

Let Y_t denote the next token at supervised position $t \in S$, and C_t the decoder prefix including task tokens and past outputs up to t . We encourage the actor to understand and utilize H by directly maximizing a conditional distributional separation regulated objective:

$$\mathcal{L}_{\text{total}} = \underbrace{\mathcal{L}_{\text{task}}}_{\text{next-token CE}} + \lambda_S \underbrace{\mathcal{L}_{\text{sep}}}_{\text{JS separation loss}} + \lambda_A \underbrace{\mathcal{L}_{\text{align}}}_{\text{plan-alignment}},$$

where $\lambda_S, \lambda_A > 0$, and $\mathcal{L}_{\text{task}}$ is the standard cross-entropy loss that ensures the model produces accurate and coherent responses based on the given task.

Conditional mind separation. In this work, we compare the full conditional distributions p_θ of the softmax of logits under matched (H) and mismatched latents (\tilde{H}) obtained by permuting latent communications across the batch. We minimize a weighted Jensen-Shannon divergence (Lin, 2002):

$$\mathcal{L}_{\text{sep}} = -\frac{1}{|S|} \sum_{t \in S} \text{JS}(p_\theta(\cdot | C_t, H), p_\theta(\cdot | C_t, \tilde{H})).$$

This objective separates matched from mismatched conditional distributions, providing a robust and efficient training signal that encourages the agent to understand and leverage the latent information.

Plan-aligned regulation. Maximizing the JS separation encourages the actor to respond to the H , but it also opens a failure mode where the model can game the objective by moving probability toward idiosyncratic tokens that increase the divergence while harming task utility. To prevent such degenerate behavior, we regularize predictions conditioned on H against those conditioned on the language-space plan (P) obtained during the generation of H . Let $p_{\text{plan}}(\cdot | C_t, P)$ denote the output distribution when only the plan is provided:

$$\mathcal{L}_{\text{align}} = \frac{1}{|S|} \sum_{t \in S} \left[\beta \text{KL}(p_\theta(\cdot | C_t, H) \| p_{\text{plan}}(\cdot | C_t, P)) + \alpha (1 - \cos(\ell_\theta(C_t, H), \ell_{\text{plan}}(C_t, P))) \right],$$

where ℓ_θ and ℓ_{plan} are the corresponding normalized logit vectors. All divergences and cosines are computed at supervised positions, probabilities are taken as softmax of logits.

Curriculum Learning. We employ a curriculum learning strategy to progressively train agents to understand the rich information embedded in latent states for communication. Inspired by (Su et al., 2025), we employ a stochastic replacement strategy that substitutes portions of latent communication with corresponding text embeddings in a left-to-right manner. Specifically, let $x_{1:L}$ be the input tokens from a reasoning model, with $e_{1:L}$ as their embeddings and $\mathbf{h}_{1:L}$ as the latent states obtained during the autoregressive generation of $x_{1:L}$. We randomly sample a replacement rate $r \sim p_R$ from a predefined uniform set $R = \{0, 0.1, \dots, 1.0\}$ and form the replaced embedding sequence by concatenation $H^{(r)} = \mathbf{h}_{1:r \times L} \oplus \mathbf{e}_{r \times L + 1:L}$ for each training instance. This method enhances training efficiency while achieving strong model performance. By integrating this curriculum, the final training objective is to minimize the following expectation over the replacement rate:

$$\mathcal{L}_{\text{total}}(\theta) = \mathbb{E}_{r \sim p_R} \left[\frac{1}{|S|} \sum_{t \in S} \left(\underbrace{-\log p_\theta(y_t | C_t, H^{(r)})}_{\mathcal{L}_{\text{task}}(t)} - \lambda_I \underbrace{\text{JS}(p_\theta(\cdot | C_t, H^{(r)}), p_\theta(\cdot | C_t, \tilde{H}))}_{\mathcal{L}_{\text{sep}}} \right) + \lambda_A \underbrace{\left[\beta \text{KL}(p_\theta(\cdot | C_t, H^{(r)}) \| p_{\text{plan}}(\cdot | C_t, P)) + \alpha (1 - \cos(\ell_\theta(C_t, H^{(r)}), \ell_{\text{plan}}(C_t, P))) \right]}_{\mathcal{L}_{\text{align}}(t)} \right].$$

3.3 INFORMATION COMPRESSION

The high-dimensional nature of latent space allows it to encode richer information than language space (Zhu et al., 2025b). We leverage this property to compress inter-agent communication. With a trained actor agent capable of understanding latent messages, we now train the reasoning agent (\mathcal{M}_ϕ) to produce shorter, more informative latent communications. Following (Hao et al., 2024; Shen et al., 2025; Cheng & Van Durme, 2024), as shown in Figure 2, we let our reasoning agent reason in a continuous latent space by autoregressive (\odot) feeding the last hidden state directly as the next input embedding, which are fully differentiable and allow for back-propagation:

$$\langle \mathcal{M}_\phi(E_i) \rightarrow h_i, \quad E_{i+1} = E_i \oplus \text{Proj}(h_i) \rangle_{\odot}, \quad (2)$$

where $\text{Proj}(\cdot)$ is a small LayerNorm+Linear bridge. We keep the actor model and communication adapter frozen and train only the reasoning model to generate compressed latents H_K by using supervisory signals derived from the actor’s cross-entropy loss and an uncertainty-weighted alignment of the actor’s output distribution under compressed to that under full length latents. A detailed description of the loss function is provided in Appendix A.

4 EXPERIMENT

Implementation Details. We implement our method based on the Qwen2.5-7B-Base and Qwen2.5-0.5B-Base models (Yang et al., 2024). All training processes are conducted using mixed-precision training (bfloat16), FlashAttention-2 (Dao, 2023), gradient checkpointing, and DeepSpeed ZeRO-2 (Rajbhandari et al., 2020) with CPU offload for parameters and optimizer states on 8 NVIDIA A100-80G GPUs with batch-level early stopping on the reasoning model. The global batch size is 16, corresponding to 2 samples per GPU. We adopt the AdamW optimizer (Loshchilov & Hutter, 2017) with a learning rate of $1e-5$, a 3% warm-up ratio. A validation split of 5% of the dataset is used for model selection. For the pre-process of latent communication, we employ a multi-head attention layer (8 heads), followed by layer normalization and an adaptive projection module. We treat the task loss with unit weight, and scale the other two terms by dynamic coefficients that are annealed during training, with Qwen2.5-7B-Base: $\lambda_{\text{sep}} \in [0.1, 2.0]$, $\lambda_{\text{align}} \in [0.1, 0.2]$ and Qwen2.5-0.5B-Base: $\lambda_{\text{sep}} \in [0.1, 0.5]$, $\lambda_{\text{align}} \in [0.1, 0.2]$. For negative sampling in the contrastive objective, we use latent communication from different tasks within the same batch, which provides a more challenging discrimination target compared to random noise.

For compression training, the weights of three losses are all 1. We implement our system with a frozen actor agent and a trainable reasoning agent based on Qwen2.5-7B-Base. Unless otherwise stated, the student is Qwen2.5-7B and the teacher All runs use mixed precision (bfloat16), FlashAttention-2 (Dao, 2023) when available, gradient checkpointing, and DeepSpeed ZeRO-2 (Rajbhandari et al., 2020) with CPU offload for parameters and optimizer states. We train on $64 \times A100-80GB$ GPUs with per-GPU micro-batch size 2; DeepSpeed automatically sets gradient accumulation to meet the target effective batch. The optimizer is AdamW with learning rate 5×10^{-5} , warmup ratio 3%, and we select models by a 5% validation split with early stopping

We choose Alfworld (Shridhar et al., 2020) to test our Interlat, which provides multi-step tasks that require a multi-agent system to plan and act based on the environment. We adopt the official split with 3119 training tasks, 140 validation tasks, and 134 test tasks. Episodes are capped at 20 environment steps; Success is 1 if the goal state is reached within the budget and 0 otherwise. All models are trained on ALFWorld trajectory data from (Song et al., 2024), which includes task descriptions, step-by-step thoughts, and actions. Latent communications are extracted from a Qwen2.5-7B-instruct and Qwen2.5-0.5B-instruct model. On our setup, the training time for the actor model is about 6

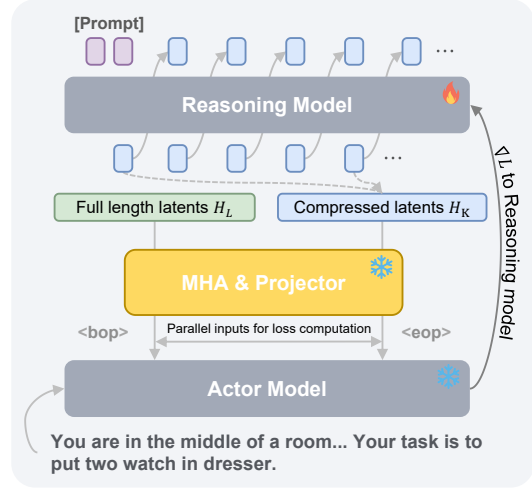


Figure 2: Training the reasoning model with frozen-actor supervision.

Method	Qwen2.5-7B-Base				Qwen2.5-0.5B-Base			
	Seen	Steps	UnSeen	Steps	Seen	Steps	UnSeen	Steps
Interlat								
Ours	70.48	9.41/12.54	65.42	9.86/13.37	61.19	10.55/14.22	57.46	9.38/13.90
Text	64.29	8.76/12.77	62.44	9.79/13.63	54.52	9.50/14.28	47.26	9.70/15.13
No-Comm	62.14	10.19/13.90	62.19	10.23/13.92	50.48	8.23/14.06	44.03	9.10/15.20
Baselines								
CoT (full)	67.14	8.15/12.04	64.93	9.02/12.87	57.86	8.30/13.23	50.75	8.94/14.39
No-CoT	65.71	8.23/12.27	62.69	9.15/13.20	57.14	8.96/13.69	50.25	9.80/14.87
Variants								
CrossTask	61.43	8.42/12.89	61.94	9.51/13.50	53.57	9.40/14.32	47.01	10.06/15.33
Noised								
CovNoise-0.5×	64.29	8.54/12.63	60.95	8.71/13.12	53.33	8.80/14.03	46.77	9.64/15.16
CovNoise-1.0×	63.81	8.66/12.76	63.68	8.72/12.82	53.10	8.96/14.14	44.53	9.68/15.40
WhiteNoise	61.90	8.65/12.97	61.19	9.32/13.46	57.38	8.00/13.11	57.21	9.18/13.81
CovGauss-0 μ	60.00	8.79/13.27	61.94	9.59/13.55	13.81	11.25/18.79	13.18	12.93/19.07
CovGauss- μ	65.71	8.58/12.50	64.93	8.63/12.62	44.52	9.21/15.20	34.33	10.19/16.63
RandomRot	57.86	8.43/13.31	63.68	9.37/13.23	59.05	8.24/13.06	51.99	9.12/14.34

Table 1: Performance of different methods and variants on seen and unseen tasks. Higher success rates indicate stronger inter-agent collaboration and task-solving ability. “Steps” reports average steps on successful tasks and average steps over all tasks, separated by a slash.

hours for 7B and 3.3 hours for 0.5B, 8 to 48 hours for the reasoning model for generating length from 8 to 128. We report the mean result over three independent runs.

Baselines and settings in Interlat. In this work, we seek to study the feasibility of agents communicating *entirely* in latent space; accordingly, we consider the following baselines: (1) **CoT (full)**. We use complete Chain-of-Thought (CoT) traces produced by a related instruction-tuned model (Qwen2.5-7B-Instruct and Qwen2.5-0.5B-Instruct) to perform full-parameter supervised fine-tuning. In inference, the model receives a complete CoT plan before generating answers. (2) **No-CoT**. The model is trained to produce the final answer directly, without receiving any plan from other agents.

We also evaluate some variants of our method: (1) **Text**. Instead of latent communication, we feed the corresponding CoT plan (in language space) to the actor. (2) **No-Comm**. We remove any communication from the actor’s input. (3) **CrossTask**. We replace the current task’s latent communication with one sampled from a different task. (4) **Noised**. We add perturbations to the latent communication H : (a) **CovNoise-0.5×/1.0×**: covariance-shaped noise $\varepsilon_t \sim \mathcal{N}(0, \hat{\Sigma})$ with optional strength $\lambda \in \{0.5, 1.0\}$, where $\hat{\Sigma}$ is the sample covariance of the original H ; (b) **WhiteNoise**: a control drawn from $\mathcal{N}(0, I)$ with the same length. (5) **CovGauss**. We replace the entire H with i.i.d. samples $H_t \sim \mathcal{N}(0, \hat{\Sigma})$ (0μ) and report a robustness check with $\mathcal{N}(\hat{\mu}, \hat{\Sigma})$ (μ). These preserve first-second order moments while removing higher-order structure and temporal alignment. (6) **RandomRot**. We apply a structure-preserving but information-scrambling transform $H' = \hat{\mu} + (H - \hat{\mu}) \hat{\Sigma}^{-1/2} Q \hat{\Sigma}^{1/2}$, where Q is a Haar-random orthogonal matrix (Mezzadri, 2006). This preserves the mean/covariance exactly while disrupting higher-order structure.

4.1 MAIN RESULT

Table 1 presents a comprehensive comparative analysis of the Interlat framework against other methods. Latent communications effectively enhance agents’ task-solving ability, as shown by the consistent improvement over fine-tuned single agent and agents trained to communicate in natural language. We describe several key findings from the experiment as follows.

Latent Communication Prompts Agent Exploration. Beyond accuracy improvements, removing the constraints of language space yields longer yet more successful trajectories for agents with latent communication. Even without explicitly training exploration policies, by effectively mind-reading other agents’ multiple plausible reasoning paths in latent communication, it naturally engages in more thorough exploratory behavior patterns. This phenomenon suggests an enhanced environmental understanding rather than random exploration, which in turn leads to higher overall task success

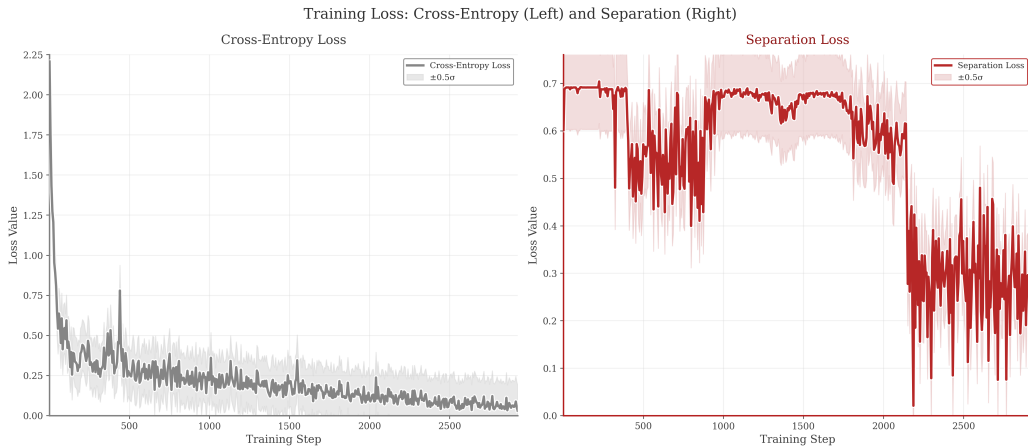


Figure 3: Training dynamics of the cross-entropy loss and separation loss: an initial plateau near 0.69 indicates no separation between matched/mismatched latents, followed by a sharp drop after $\sim 2.2k$ steps, marking the model’s “aha” moment in exploiting task-relevant latent information.

rates than agents with a natural language plan with fewer steps. A deeper analysis of the relationship between step counts and success rates is provided in the Appendix C.

Actor Agent Actually Comprehends Latent Communication. With dense and implicit information in the latent space, we test whether the trained actor agent genuinely exploits the latent information carried by latent communication, rather than matching superficial distributional cues. As shown in Table 1, replacing task-specific latents with cross-task mismatch latents causes a substantial accuracy drop. Although these foreign messages share similar global statistics, they encode reasoning paths irrelevant to the current task. Accuracy declines further when we substitute covariance-matched Gaussian surrogates or apply random orthogonal rotations to latents, variances that preserve first- and second-order moments while disrupting structure. Performance also drops under additive noise to the original latents, which hampers the extraction of the information. White noise, which contains no structured content, also impairs performance. Overall, these variances indicate that successful execution depends on understanding both the meaningful, task-specific information and the inherent structure of the latent communication, which represents constructed reasoning paths.

An ‘Aha’ Moment in Understanding Latent Information. Learning to interpret latent communication aligns with an LLM’s inherent processing modality, as these models are pre-trained on natural language but internally process information using hidden states. Through curriculum learning and tailored loss functions, we guide LLMs to gradually comprehend latent information. As shown in Figure 3, the separation loss reveals a distinct two-phase learning curve. For the first 2,200 steps, the loss plateaus near 0.69, which is the maximum Jensen-Shannon divergence, indicating an inability to distinguish task-specific from cross-batch latent messages. Around step 2,200, however, the loss drops sharply, indicating a qualitative leap in the model’s “mind-reading” capacity. This transition reflects the emergence of a genuine understanding of latent information for task solving. Notably, using cross-batch messages as negatives poses a more significant challenge than using random noise, as they are coherent yet task-irrelevant. The model’s ability to achieve eventual discrimination underscores its move beyond superficial patterns toward meaningful latent communication.

4.2 COMPRESSION

Compression Analysis. Theoretically, with a much higher expressive range, latent communications can encode rich information in far fewer positions than natural-language tokens. To quantify their compression capacity, we evaluate both the compression process on the latent communications from training-free Qwen-2.5B-Instruct model and training settings on a compression-trained Qwen2.5-7B-Base model.

Ratio	Seen	Unseen	Time	Ratio	Seen	Unseen	Time
Untrained				Untrained			
Full	70.48 \pm 1.01	<u>65.42</u> \pm 0.87	9.19s	128L	64.55 \pm 2.26	60.25 \pm 2.06	3.55s
90%	68.57 \pm 1.63	67.16 \pm 1.97	-	64L	66.23 \pm 1.95	61.53 \pm 4.32	1.83s
80%	68.10 \pm 1.83	61.69 \pm 1.43	-	32L	63.57 \pm 2.01	60.18 \pm 3.58	1.03s
70%	67.14 \pm 1.82	63.43 \pm 2.24	-	16L	64.29 \pm 1.34	60.00 \pm 3.01	0.62s
60%	66.43 \pm 1.63	59.20 \pm 3.69	-	8L	64.00 \pm 2.18	57.46 \pm 2.69	0.39s
50%	72.14 \pm 1.48	61.19 \pm 2.84	-	Trained			
40%	66.90 \pm 2.31	59.95 \pm 2.64	-	128L	68.10 \pm 1.93	62.94 \pm 2.03	2.25s
30%	65.95 \pm 2.12	62.19 \pm 1.58	-	64L	<u>67.14</u> \pm 1.56	<u>61.94</u> \pm 2.13	1.16s
20%	67.86 \pm 3.23	61.44 \pm 1.58	-	32L	66.90 \pm 1.46	61.94 \pm 2.56	0.60s
10%	67.86 \pm 2.12	62.44 \pm 2.64	-	16L	66.43 \pm 2.05	61.69 \pm 2.56	0.33s
5%	64.29 \pm 1.12	60.95 \pm 1.35	-	8L	66.43 \pm 1.22	60.45 \pm 2.23	0.20s
0%	62.14 \pm 2.01	62.14 \pm 2.32	-				

Table 2: Result of compression on seen and unseen tasks. **Left:** training-free sweep over retained ratio R from full to zero. **Right:** varying the length of transmitted latents $L \in \{8, 16, 32, 64, 128\}$ for training-free and trained reasoning models. Time denotes end-to-end latency (s) of the message generation process. The top scores are in **bold**, with the second-highest underlined.

As shown in Table 2, under the training-free setting, Interlat achieves optimal performance at 50% compression with a success rate of 72.14%, even surpassing the uncompressed baseline. This suggests that moderate compression preserves essential information while reducing computational overhead. However, performance becomes volatile at extreme compression ratios around 20% compression, indicating sensitivity to extreme compression ratios. When hidden states are completely removed, accuracy drops to 62.14%, confirming their critical role in information transmission. Under the training setting, we apply various compression rates to the reasoning model, generating latent communications of 8, 16, 32, 64, and 128 hidden states ($\approx 1.8\%$, 3.6% , 7.2% , 14.4% , and 28.8% of the full sequence length, respectively) for the action agent. This compression training process yields more stable performance and higher success rates across various compression levels, demonstrating the model’s ability to learn efficient, compressed representations.

Furthermore, compression markedly improves wall-clock efficiency. By generating far fewer hidden states for inter-agent communication, the average end-to-end latency drops from 9.19 s at full length to 0.39 s with an 8-step latents, a nearly $24\times$ speed-up. Although with a lightweight bridge module, the trained reasoning agent further reduces the generation runtime to 0.20s by largely eliminating the decode-re-encode overhead inherent in token-based communication.

Why compression is effective. To understand the mechanisms that make compression effective, we first measure its impact on predictive uncertainty by sweeping the communication rate $R \in [0, 1]$ and computing the cross-entropy (CE, in bits/hidden state). Define CE_{full} as the CE under full communication, and $CE_{comp}(R)$ as the CE at rate R . We report the task-averaged relative change $\Delta CE\%(R) = 100 \times \frac{CE_{comp}(R) - CE_{full}}{CE_{full}}$. Figure 5 reveals several key insights: (1) $\Delta CE\%$ decreases monotonically with increasing R , exhibiting a plateau region from approximately 30% to 75% bits/hidden state, which corresponds to the range of optimal performance; (2) the trained latent communication curve consistently outperforms the training-free curve across all compression rates, with the vertical gap reaching a maximum of approxi-

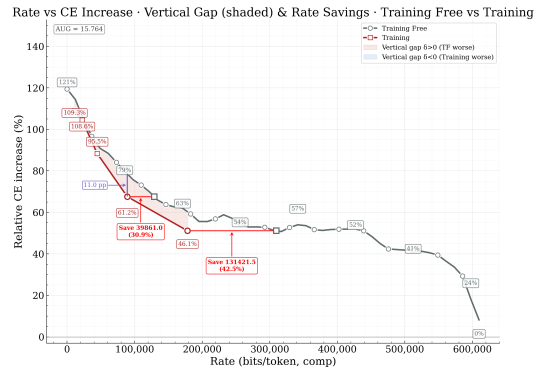


Figure 5: The task-averaged relative change ΔCE and the relative saving rates before and after the compression training process.

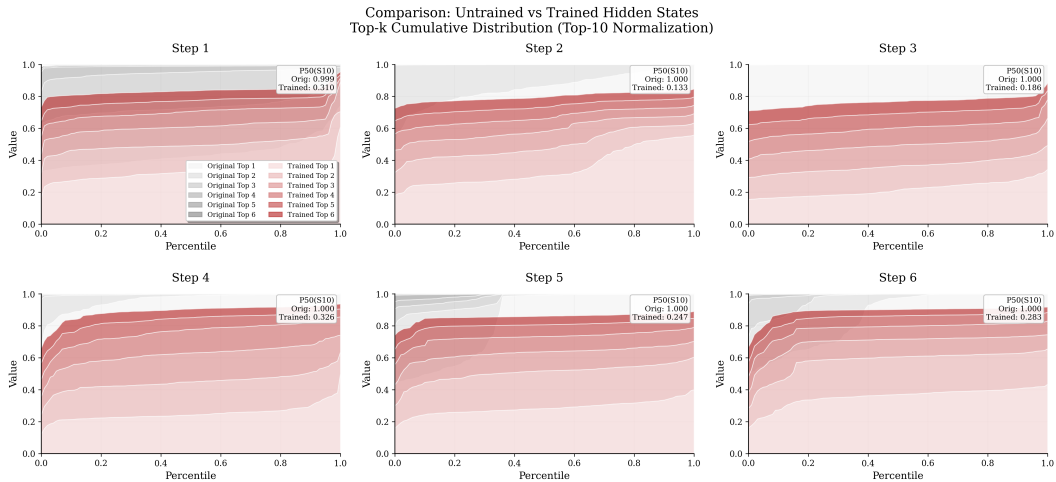


Figure 4: Analysis of parallelism in latent communication across the first six steps. The **red** denotes latents from the trained model, and the **gray** is the untrained model. Trained latents retain stable vertical gaps between successive Top- k bands and exhibit markedly lower $P_{50}(S_{10})$, indicating persistent parallelism, whereas the untrained latents progressively collapse toward Top-1.

Actor	Seen	Unseen
Ours Full	70.48 \pm 1.01	65.42 \pm 0.87
w/o curri	33.10 \pm 2.97	20.65 \pm 2.15
w/o \mathcal{L}_{sep}	58.81 \pm 1.41	60.70 \pm 5.50
w/o \mathcal{L}_{align}	56.90 \pm 1.41	53.98 \pm 3.35
w/o adapter	4.05 \pm 1.70	4.48 \pm 1.31

Reasoning	Seen	Unseen
Ours Full	68.10 \pm 1.93	62.94 \pm 2.03
w/o \mathcal{L}_{task}	65.71 \pm 1.43	63.18 \pm 3.47
w/o \mathcal{L}_{pref}	64.76 \pm 2.97	60.20 \pm 3.13
w/o \mathcal{L}_{geom}	64.05 \pm 3.55	59.45 \pm 3.01

Table 3: Ablation of training components. See Appendix C for full results and analysis.

mately 11 percentage points; (3) the trained reasoning agent achieves substantial computational savings-up to 131,421.5 rates (42.5% reduction) at optimal compression points while maintaining competitive performance.

We further examine how information is preserved under compression. The probability distribution serves as the model’s implicit *information parallelism budget*, estimating how many viable possibilities are preserved at each step. Figure 4 shows the parallelism of the reasoning agent’s latent communication by examining the first six hidden states, each representing a distinct reasoning step. For each step, we compute the output probability distribution from the language model (LM) head and plot the cumulative probability mass of the top- k tokens ($k = 1 \dots 6$) across communication percentiles and renormalize within top-10 steps. Steps in latents from the trained reasoning agent exhibits stable vertical gaps between successive top- k curves across steps, indicating persistent parallelism rather than the progressive convergence observed in the untrained model. Furthermore, we measure head coverage using $P_{50}(S_{10})$, defined as the median probability mass of the top-10 tokens ($S_{10} = \sum_{i=1}^{10} p(i)$) across the communication. The trained model shows a significantly lower $P_{50}(S_{10})$, suggesting that the trained model preserves a broader set of plausible reasoning paths within a compressed latent representation. These results demonstrate that the trained model sustains diverse parallel exploration over multiple reasoning steps, avoiding premature collapse into a single hypothesis in communications. This capability enables the model to retain richer information for downstream tasks. A detailed results with extended step-wise results over additional steps is provided in Appendix E.

4.3 ABLATION STUDIES

To assess the contribution of each training component, we performed a systematic ablation study on both the actor and reasoning models. The results, summarized in Table 3, confirm that each component is crucial for achieving optimal performance.

For the actor model, removing curriculum learning forces the model to interpret latent communications from scratch, leading to extremely unstable training dynamics and severely degraded comprehension, as illustrated in Figure 6. Removing the separation loss induces shortcut behavior; the model learns to ignore the latent communication and rely only on the textual task prompt, causing performance to regress toward the single agent baseline. Removing the communication adapter causes the largest drop; despite generating fluent and coherent responses, the model fails to complete tasks, underscoring the adapter’s role in bridging the agents’ latent spaces and enabling interpretation of latent communications.

For the reasoning model, which is trained to generate compressed latents, we ablated its three core loss functions with compressed target length $K = 128$. The most critical component is the latent direction alignment loss ($\mathcal{L}_{\text{geom}}$). This highlights the importance of maintaining geometric consistency between the compressed latents and the uncompressed ones. The uncertainty-weighted agreement loss ($\mathcal{L}_{\text{pref}}$) is also vital, as removing it significantly impairs the model’s ability to produce latents that elicit the correct behavior from the actor. Interestingly, removing the actor’s cross-entropy loss ($\mathcal{L}_{\text{task}}$) slightly improves performance on unseen tasks, from 62.05 to 62.90, suggesting that while directly optimizing for the frozen actor’s outputs is beneficial for in-distribution tasks, it may cause minor overfitting that slightly hinders generalization. We leave a deeper investigation into this trade-off to future work.

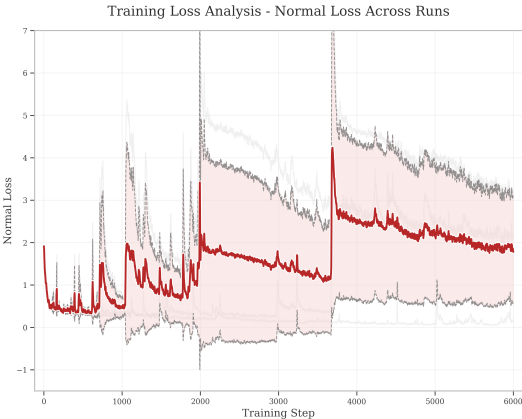


Figure 6: Training dynamics of the cross entropy loss when removing curriculum learning.

5 CONCLUSION

In this paper, we presented Interlat, a novel paradigm for inter-agent communication entirely in latent space. Through extensive experiments, we demonstrated that Interlat successfully enhances agents’ task-solving ability and communication efficiency over language-based methods by effectively utilizing task-related latent information. Analysis also highlighted how latent messages can be highly compressed while retaining performance by preserving diverse, parallel reasoning paths. Future work can further explore the integration of models from different families and leveraging hidden states from multiple layers to enable richer, more insightful communication. Another promising direction is joint training of more agents to communicate in latent space, which has the potential to scale our method. We anticipate these findings will encourage broader study into latent space communication and contribute to the development of more advanced multi-agent systems.

REFERENCES

- Hillel Aviezer, Yaacov Trope, and Alexander Todorov. Body cues, not facial expressions, discriminate between intense positive and negative emotions. *Science*, 338(6111):1225–1229, 2012. doi: 10.1126/science.1224313. URL <https://www.science.org/doi/abs/10.1126/science.1224313>.
- Sangmin Bae, Adam Fisch, Hrayr Harutyunyan, Ziwei Ji, Seungyeon Kim, and Tal Schuster. Relaxed recursive transformers: Effective parameter sharing with layer-wise lora. *arXiv preprint arXiv:2410.20672*, 2024.

-
- Mert Cemri, Melissa Z Pan, Shuyi Yang, Lakshya A Agrawal, Bhavya Chopra, Rishabh Tiwari, Kurt Keutzer, Aditya Parameswaran, Dan Klein, Kannan Ramchandran, et al. Why do multi-agent llm systems fail? *arXiv preprint arXiv:2503.13657*, 2025.
- Yanda Chen, Joe Benton, Ansh Radhakrishnan, Jonathan Uesato, Carson Denison, John Schulman, Arushi Somani, Peter Hase, Misha Wagner, Fabien Roger, et al. Reasoning models don't always say what they think. *arXiv preprint arXiv:2505.05410*, 2025.
- Jeffrey Cheng and Benjamin Van Durme. Compressed chain of thought: Efficient reasoning through dense representations. *arXiv preprint arXiv:2412.13171*, 2024.
- Tri Dao. Flashattention-2: Faster attention with better parallelism and work partitioning. *arXiv preprint arXiv:2307.08691*, 2023.
- Paul C Fletcher, Francesca Happe, Uta Frith, Simon C Baker, Ray J Dolan, Richard SJ Frackowiak, and Chris D Frith. Other minds in the brain: a functional imaging study of "theory of mind" in story comprehension. *Cognition*, 57(2):109–128, 1995.
- Yihang Gao, Chuanyang Zheng, Enze Xie, Han Shi, Tianyang Hu, Yu Li, Michael K Ng, Zhenguo Li, and Zhaoqiang Liu. Algoformer: An efficient transformer framework with algorithmic structures. *arXiv preprint arXiv:2402.13572*, 2024.
- Jonas Geiping, Sean McLeish, Neel Jain, John Kirchenbauer, Siddharth Singh, Brian R Bartoldson, Bhavya Kailkhura, Abhinav Bhatele, and Tom Goldstein. Scaling up test-time compute with latent reasoning: A recurrent depth approach. *arXiv preprint arXiv:2502.05171*, 2025.
- Sachin Goyal, Ziwei Ji, Ankit Singh Rawat, Aditya Krishna Menon, Sanjiv Kumar, and Vaishnavh Nagarajan. Think before you speak: Training language models with pause tokens. *arXiv preprint arXiv:2310.02226*, 2023.
- Shibo Hao, Sainbayar Sukhbaatar, DiJia Su, Xian Li, Zhiting Hu, Jason Weston, and Yuandong Tian. Training large language models to reason in a continuous latent space. *arXiv preprint arXiv:2412.06769*, 2024.
- Spencer D Kelly, Aslı Özyürek, and Eric Maris. Two sides of the same coin: Speech and gesture mutually interact to enhance comprehension. *Psychological science*, 21(2):260–267, 2010.
- Jianhua Lin. Divergence measures based on the shannon entropy. *IEEE Transactions on Information theory*, 37(1):145–151, 2002.
- Luyang Liu, Jonas Pfeiffer, Jiaying Wu, Jun Xie, and Arthur Szlam. Deliberation in latent space via differentiable cache augmentation. *arXiv preprint arXiv:2412.17747*, 2024.
- Ilya Loshchilov and Frank Hutter. Decoupled weight decay regularization. *arXiv preprint arXiv:1711.05101*, 2017.
- Francesco Mezzadri. How to generate random matrices from the classical compact groups. *arXiv preprint math-ph/0609050*, 2006.
- Jacob Pfau, William Merrill, and Samuel R Bowman. Let's think dot by dot: Hidden computation in transformer language models. *arXiv preprint arXiv:2404.15758*, 2024.
- Chau Pham, Boyi Liu, Yingxiang Yang, Zhengyu Chen, Tianyi Liu, Jianbo Yuan, Bryan A Plummer, Zhaoran Wang, and Hongxia Yang. Let models speak ciphers: Multiagent debate through embeddings. *arXiv preprint arXiv:2310.06272*, 2023.
- Chen Qian, Zihao Xie, Yifei Wang, Wei Liu, Kunlun Zhu, Hanchen Xia, Yufan Dang, Zhuoyun Du, Weize Chen, Cheng Yang, et al. Scaling large language model-based multi-agent collaboration. *arXiv preprint arXiv:2406.07155*, 2024.
- Samyam Rajbhandari, Jeff Rasley, Olatunji Ruwase, and Yuxiong He. Zero: Memory optimizations toward training trillion parameter models. In *SC20: International Conference for High Performance Computing, Networking, Storage and Analysis*, pp. 1–16. IEEE, 2020.

-
- Vignav Ramesh and Kenneth Li. Communicating activations between language model agents. *arXiv preprint arXiv:2501.14082*, 2025.
- Zhenyi Shen, Hanqi Yan, Linhai Zhang, Zhanghao Hu, Yali Du, and Yulan He. Codi: Compressing chain-of-thought into continuous space via self-distillation. *arXiv preprint arXiv:2502.21074*, 2025.
- Mohit Shridhar, Xingdi Yuan, Marc-Alexandre Côté, Yonatan Bisk, Adam Trischler, and Matthew Hausknecht. Alfworld: Aligning text and embodied environments for interactive learning. *arXiv preprint arXiv:2010.03768*, 2020.
- Yifan Song, Da Yin, Xiang Yue, Jie Huang, Sujian Li, and Bill Yuchen Lin. Trial and error: Exploration-based trajectory optimization for llm agents. *arXiv preprint arXiv:2403.02502*, 2024.
- DiJia Su, Hanlin Zhu, Yingchen Xu, Jiantao Jiao, Yuandong Tian, and Qingqing Zheng. Token assorted: Mixing latent and text tokens for improved language model reasoning. *arXiv preprint arXiv:2502.03275*, 2025.
- Yichen Tang, Weihang Su, Yujia Zhou, Yiqun Liu, Min Zhang, Shaoping Ma, and Qingyao Ai. Augmenting multi-agent communication with state delta trajectory. *arXiv preprint arXiv:2506.19209*, 2025.
- Khanh-Tung Tran, Dung Dao, Minh-Duong Nguyen, Quoc-Viet Pham, Barry O’Sullivan, and Hoang D Nguyen. Multi-agent collaboration mechanisms: A survey of llms. *arXiv preprint arXiv:2501.06322*, 2025.
- Kai Vogeley, Patrick Bussfeld, Albert Newen, Sylvie Herrmann, Francesca Happé, Peter Falkai, Wolfgang Maier, Nadim Joni Shah, Gereon R Fink, and Karl Zilles. Mind reading: neural mechanisms of theory of mind and self-perspective. *Neuroimage*, 14(1):170–181, 2001.
- Lei Wang, Chen Ma, Xueyang Feng, Zeyu Zhang, Hao Yang, Jingsen Zhang, Zhiyuan Chen, Jiakai Tang, Xu Chen, Yankai Lin, et al. A survey on large language model based autonomous agents. *Frontiers of Computer Science*, 18(6):186345, 2024.
- Yingxu Wang, Siwei Liu, Jinyuan Fang, and Zaiqiao Meng. Evoagentx: An automated framework for evolving agentic workflows. *arXiv preprint arXiv:2507.03616*, 2025.
- Jason Wei, Xuezhi Wang, Dale Schuurmans, Maarten Bosma, Fei Xia, Ed Chi, Quoc V Le, Denny Zhou, et al. Chain-of-thought prompting elicits reasoning in large language models. *Advances in neural information processing systems*, 35:24824–24837, 2022.
- An Yang, Baosong Yang, Beichen Zhang, Binyuan Hui, Bo Zheng, Bowen Yu, Chengyuan Li, Dayiheng Liu, Fei Huang, Haoran Wei, Huan Lin, Jian Yang, Jianhong Tu, Jianwei Zhang, Jianxin Yang, Jiayi Yang, Jingren Zhou, Junyang Lin, Kai Dang, Keming Lu, Keqin Bao, Kexin Yang, Le Yu, Mei Li, Mingfeng Xue, Pei Zhang, Qin Zhu, Rui Men, Runji Lin, Tianhao Li, Tingyu Xia, Xingzhang Ren, Xuancheng Ren, Yang Fan, Yang Su, Yichang Zhang, Yu Wan, Yuqiong Liu, Zeyu Cui, Zhenru Zhang, and Zihan Qiu. Qwen2.5 technical report. *arXiv preprint arXiv:2412.15115*, 2024.
- Fei Yu, Hongbo Zhang, Prayag Tiwari, and Benyou Wang. Natural language reasoning, a survey. *ACM Computing Surveys*, 56(12):1–39, 2024.
- Guibin Zhang, Yanwei Yue, Zhixun Li, Sukwon Yun, Guancheng Wan, Kun Wang, Dawei Cheng, Jeffrey Xu Yu, and Tianlong Chen. Cut the crap: An economical communication pipeline for llm-based multi-agent systems. *arXiv preprint arXiv:2410.02506*, 2024a.
- Jiayi Zhang, Jinyu Xiang, Zhaoyang Yu, Fengwei Teng, Xionghui Chen, Jiaqi Chen, Mingchen Zhuge, Xin Cheng, Sirui Hong, Jinlin Wang, et al. Aflow: Automating agentic workflow generation. *arXiv preprint arXiv:2410.10762*, 2024b.
- Kunlun Zhu, Hongyi Du, Zhaochen Hong, Xiaocheng Yang, Shuyi Guo, Zhe Wang, Zhenhailong Wang, Cheng Qian, Xiangru Tang, Heng Ji, et al. Multiagentbench: Evaluating the collaboration and competition of llm agents. *arXiv preprint arXiv:2503.01935*, 2025a.

Rui-Jie Zhu, Tianhao Peng, Tianhao Cheng, Xingwei Qu, Jinfan Huang, Dawei Zhu, Hao Wang, Kaiwen Xue, Xuanliang Zhang, Yong Shan, et al. A survey on latent reasoning. *arXiv preprint arXiv:2507.06203*, 2025b.

Appendix

The supplementary information accompanying the main paper provides additional data, explanations, and details.

A COMPRESSION LOSS

Setup. After training an actor A_θ to *consume* latent communications, we freeze A_θ and train a reasoning model M_ϕ to *produce* compact, information-dense latent communications of length K that the frozen actor can still exploit. For an input instance with supervised token indices S (the teacher-forced window after the first user turn), let

$$H_{1:K}^{\text{gen}} = M_\phi(x) \quad \text{and} \quad H_{1:L}^{\text{full}} = M_{\text{ins}}(x),$$

denote respectively the *generated* latent communication from the trainable reasoning model and the full-length latent communication extracted from a fixed instruction-tuned model M_{ins} . A lightweight communication adapter $g(\cdot)$ (kept frozen) *preprocesses* the latent communication before concatenation with boundary tokens $\langle \text{bop} \rangle / \langle \text{eop} \rangle$. For brevity, we use $H_K \equiv H_{1:K}^{\text{gen}}$ and $H_L \equiv H_{1:L}^{\text{full}}$.

We define three *actor-scored* forward paths through the frozen actor A_θ given a prompt x : (i) **Path A (generated latents)**: $E^{(A)} = [e(x), e(\langle \text{bop} \rangle), g(H_K), e(\langle \text{eop} \rangle)]$; (ii) **Path D (full-length latents)**: $E^{(D)} = [e(x), e(\langle \text{bop} \rangle), g(H_L), e(\langle \text{eop} \rangle)]$; (iii) **Path B (no latents)**: $E^{(B)} = [e(x)]$. Let $\ell_t^{(q)}$ be the frozen-actor logits at position $t \in S$ under path $q \in \{A, D, B\}$, and

$$p_t^{(q)} = \text{softmax}(\ell_t^{(q)} / T)$$

be the corresponding token distributions with temperature $T \geq 1$ used for distillation. Unless stated otherwise, gradients do not flow into A_θ or $g(\cdot)$.

(1) Actor cross-entropy utility. We require the generated message to be *useful* for the frozen actor:

$$\mathcal{L}_{\text{task}} = \frac{1}{|S|} \sum_{t \in S} (-\log p_\theta(y_t | C_t, H_K)) \quad (\text{computed under Path A}).$$

This term enforces that the compressed latents H_K still drive correct next-token predictions, directly penalizing information loss due to shortening ($K \ll L$). It prevents degenerate ‘‘over-compression’’ that would be efficient but useless to the actor. Practically, it anchors training on task utility so that any compression gain does not come at the cost of downstream performance.

(2) Uncertainty-weighted agreement. We further encourage *behavioral agreement* between using full-length latent communication (Path D) and generated compressed latent communication (Path A), with per-token weights that reflect how much *any* latent reduces uncertainty relative to the no-latent baseline (Path B). Let the entropies be

$$H^{(q)}(t) = - \sum_v p_t^{(q)}(v) \log p_t^{(q)}(v), \quad q \in \{A, D, B\}.$$

Define raw weights $w_t^* = \max(H^{(B)}(t) - H^{(D)}(t), 0)$ and optionally clip w_t^* to $[0, \tau]$ to suppress outliers. Normalize to unit mean:

$$w_t = \frac{w_t^*}{\frac{1}{|S|} \sum_{u \in S} w_u^* + \varepsilon}.$$

The agreement term is a temperature-scaled KL:

$$\mathcal{L}_{\text{pref}} = \frac{1}{\sum_{t \in S} w_t} \sum_{t \in S} w_t T^2 \text{KL}(p_t^{(D)} \| p_t^{(A)}) = \frac{T^2}{\sum_{t \in S} w_t} \sum_{t \in S} w_t \sum_v p_t^{(D)}(v) \log \frac{p_t^{(D)}(v)}{p_t^{(A)}(v)}.$$

By matching $p^{(A)}$ to $p^{(D)}$ where full latents actually reduce uncertainty (weights w_t), this term teaches H_K to reproduce the *informative* behavioral effects of H_L while ignoring positions where latents are unhelpful.

(3) Latent direction alignment. To stabilize compression, we align the *global direction* of actor-side latent features induced by generated vs. data latents. Let $Z_k^{(q)} \in \mathbb{R}^{d_z}$ be the actor-side features (after $g(\cdot)$ and the actor’s input stack) at latent step k under path $q \in \{A, D\}$. When H_L has length $L \neq K$, apply a fixed resampling operator ρ_K (e.g., uniform down/up-sampling) and write $Z_{1:K}^{(D)} = \rho_K(Z_{1:L}^{(D)})$. Define step-averaged directions $\bar{z}^{(q)} = \frac{1}{K} \sum_{k=1}^K Z_k^{(q)}$ and the cosine penalty

$$\mathcal{L}_{\text{geom}} = 1 - \cos(\bar{z}^{(A)}, \bar{z}^{(D)}) = 1 - \frac{\langle \bar{z}^{(A)}, \bar{z}^{(D)} \rangle}{\|\bar{z}^{(A)}\|_2 \|\bar{z}^{(D)}\|_2}.$$

This term preserves the *geometry* of the actor-side representations, preventing the compressed latents from drifting to directions that the actor interprets differently. Empirically, it improves stability and mitigates mode collapse when K is small by retaining the global semantic orientation of H_L .

Overall objective. The compression objective for M_ϕ (with A_θ frozen) is

$$\mathcal{L}_{\text{compress}} = \lambda_{\text{task}} \mathcal{L}_{\text{task}} + \lambda_{\text{pref}} \mathcal{L}_{\text{pref}} + \lambda_{\text{geom}} \mathcal{L}_{\text{geom}}.$$

In practice, all terms are computed over $t \in S$ with teacher forcing; gradients propagate only to ϕ .

B BENCHMARK

Alfworld (Shridhar et al., 2020) is a text-only benchmark that simulates embodied household tasks while keeping interaction purely in natural language. Agents observe textual descriptions of the scene and issue high-level commands from a constrained action set (e.g., go to, open, close, take, put, toggle on/off, heat, cool, examine). Tasks are long-horizon and compositional, requiring perception, planning, and execution over multiple steps under partial observability. The benchmark provides official train/validation/test splits and a standard success metric under a fixed step budget (e.g., 20 steps in our setup), enabling systematic and reproducible evaluation of sequential decision-making.

Why ALFWorld for this work? First, its multi-step, plan-then-act structure closely matches our sender-receiver setup and stresses the precise abilities our method targets: exploration quality, plan following, and coordination. **Prior work shows that continuous latent reasoning is especially advantageous on planning-heavy tasks**, latent representations preserve multiple candidate reasoning branches and promote breadth-first search (BFS) dynamics (Hao et al., 2024). **We ask whether the same or similar advantages hold when agents communicate in latent space**; ALFWorld is an ideal testbed because its tasks require long-horizon planning, where agents iteratively observe, form thoughts, and act based on environment feedback. Second, the text-only interface isolates the communication modality itself, letting us cleanly contrast language space vs. latent space communication without confounds from external tools or perception pipelines, thereby allowing us to probe what new properties latent communication introduces for agent behavior. Third, community resources provide consistent task descriptions and action trajectories, allowing us to derive both language baselines (e.g., a CoT plan) and latent representations from the same underlying data, reducing distribution shift. Finally, the moderate episode length and standardized protocol make it feasible to average over multiple independent runs, yielding robust statistics for ablations and compression analyses.

C ABLATIONS AND STEP ANALYSIS

We present ablation studies for both the actor and reasoning models, reporting average steps for successful trials versus all trials (success/all). As a complement to our main ablation results, this section analyzes the step count to provide deeper insights into agent behavior.

As shown in Table 4, the results reveal a nuanced relationship between step count and performance. On seen tasks, ablating components results in a lower overall success rate. Interestingly, although these models take fewer steps on the trials they do complete, their high failure rate indicates an inability to properly interpret the latent communication and reliably solve tasks. These results support our findings that information-rich latent communication encourages more effective and thorough exploration.

Method	Seen	Steps	Unseen	Steps
Actor model				
Ours Full	70.48 \pm 1.01	9.41/12.54	65.42 \pm 0.87	9.86/13.37
w/o curri	33.10 \pm 2.97	9.07/16.38	20.65 \pm 2.15	10.47/18.03
w/o \mathcal{L}_{sep}	<u>58.81</u> \pm 1.41	8.07/12.98	<u>60.70</u> \pm 5.50	9.64/13.71
w/o $\mathcal{L}_{\text{align}}$	56.90 \pm 1.41	8.16/13.26	53.98 \pm 3.35	9.56/14.36
w/o adapter	4.05 \pm 1.70	9.32/19.57	4.48 \pm 1.31	10.53/19.58
Reasoning model				
Ours Full	68.10 \pm 1.93	9.21/12.65	<u>62.94</u> \pm 2.03	9.88/13.63
w/o $\mathcal{L}_{\text{task}}$	<u>65.71</u> \pm 1.43	8.86/12.68	63.18 \pm 3.47	9.68/13.48
w/o $\mathcal{L}_{\text{pref}}$	64.76 \pm 2.97	8.92/12.82	60.20 \pm 3.13	9.68/13.79
w/o $\mathcal{L}_{\text{geom}}$	64.05 \pm 3.55	8.71/12.77	59.45 \pm 3.01	9.88/13.98

Table 4: Ablation of training components. ‘‘Ours Full’’ uses all components.

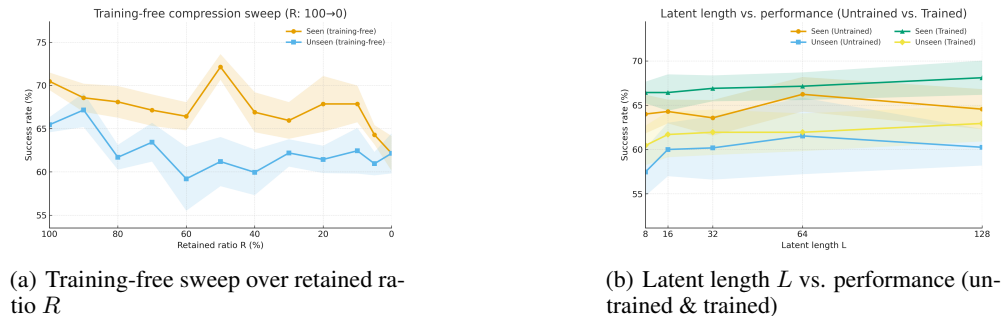


Figure 7: Result of compression on seen and unseen tasks. **Left:** Success rate under training-free compression with different retained ratios R . **Right:** Performance of untrained and trained models across latent lengths L

On unseen tasks, several ablations (*e.g.*, removing the curriculum or the adapter) exhibit an opposite pattern: the agent takes more steps yet achieves a lower success rate. This demonstrates that longer trajectories do not necessarily equate to productive exploration. Without these crucial components, the agent’s policy tends to wander without forming effective task-solving strategies. Therefore, the additional steps reflect an unstructured, inefficient search rather than the deliberate exploration enabled by our method. This analysis underscores the importance of evaluating step count in conjunction with the success rate for a holistic assessment of an agent’s true performance.

D COMPRESSION RESULT

In this section, we provide more detailed results on compression with average steps as success/all across tasks in Table 5 and corresponding performance trend in Figure 7. Latency is measured on the same machine and decoding policy (if needed) across rows ¹.

E LATENT PARALLELISM ANALYSIS

We first compared the latent communications produced by our trained reasoning model with those from an off-the-shelf Qwen2.5-7B-Instruct model in the compression-effectiveness analysis (see

¹For the untrained reasoning model, we use the standard generate API from Hugging Face transformers; see <https://github.com/huggingface/transformers>.

Ratio	Seen	Steps	Unseen	Steps	Time
Untrained					
Full	70.48 \pm 1.01	9.41/12.54	65.42 \pm 0.87	9.86/13.37	9.19s
90%	68.57 \pm 1.63	8.77/12.30	67.16 \pm 1.97	9.27/12.79	-
80%	68.10 \pm 1.83	8.56/12.21	61.69 \pm 1.43	9.10/13.28	-
70%	67.14 \pm 1.82	8.68/12.40	63.43 \pm 2.24	9.42/13.29	-
60%	66.43 \pm 1.63	8.52/12.37	59.20 \pm 3.69	9.90/14.02	-
50%	72.14 \pm 1.48	9.03/12.09	61.19 \pm 2.84	9.37/13.50	-
40%	66.90 \pm 2.31	8.88/12.56	59.95 \pm 2.64	9.52/13.72	-
30%	65.95 \pm 2.12	8.80/12.61	62.19 \pm 1.58	10.11/13.85	-
20%	67.86 \pm 3.23	8.97/12.52	61.44 \pm 1.58	9.98/13.84	-
10%	67.86 \pm 2.12	8.76/12.37	62.44 \pm 2.64	9.72/13.58	-
5%	64.52 \pm 1.12	9.19/13.02	60.95 \pm 1.35	9.90/13.84	-
0%	62.14 \pm 2.01	10.19/13.90	62.19 \pm 2.32	10.23/13.92	-
128L	64.52 \pm 2.26	8.68/12.70	60.20 \pm 2.06	9.69/13.79	3.55s
64L	66.19 \pm 1.95	8.76/12.56	61.44 \pm 4.32	9.85/13.76	1.83s
32L	63.57 \pm 2.01	8.66/12.79	60.20 \pm 3.58	9.87/13.90	1.03s
16L	64.29 \pm 1.34	8.64/12.70	59.95 \pm 3.01	10.07/14.05	0.62s
8L	64.05 \pm 2.18	8.80/12.83	57.46 \pm 2.69	10.29/14.42	0.39s
Trained					
128L	68.10 \pm 1.93	9.21/12.65	62.94 \pm 2.03	9.88/13.63	2.25s
64L	67.14 \pm 1.56	9.15/12.72	61.94 \pm 2.13	9.92/13.76	1.16s
32L	66.90 \pm 1.46	9.02/12.65	61.94 \pm 2.56	9.96/13.78	0.60s
16L	66.43 \pm 2.05	9.08/12.75	61.69 \pm 2.56	9.98/13.82	0.33s
8L	66.43 \pm 1.22	9.11/12.77	60.45 \pm 2.23	9.90/13.89	0.20s

Table 5: Complete compression results with seen/unseen accuracy, steps, and latency across tasks.

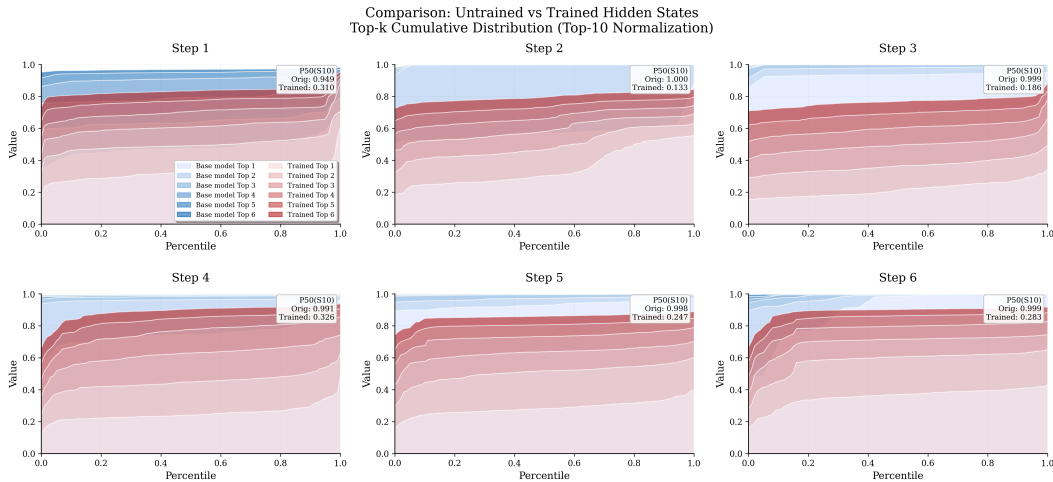


Figure 8: Parallelism in latent communication over the first six steps. Red indicates latents from the trained model, and blue indicates latents from the untrained base model. The trained latents preserve stable vertical gaps between successive Top- k bands and achieve a markedly lower $P_{50}(S_{10})$, evidencing persistent parallelism, whereas the untrained base model’s latents progressively collapse toward Top-1.

the Experiments section). Because our reasoning model is initialized from Qwen2.5-7B-Base, we additionally compare it with this base model, which has not been trained for generating compressed latent communication, in Figure 8. The findings are consistent with the earlier comparison: the trained

model maintains stable vertical gaps between successive Top- k curves across steps and exhibits a substantially lower $P_{50}(S_{10})$, whereas the base model shows a clear convergence toward Top-1.

We further extend the parallelism analysis to a deeper horizon of 32 steps. As shown in Figure 9, the trained model exhibits stable vertical gaps between successive Top- k curves throughout these steps. This extended analysis further verifies that the trained latent representations preserve a broader set of plausible reasoning paths by sustaining a more balanced probability distribution rather than prematurely collapsing to a Top-1 hypothesis.

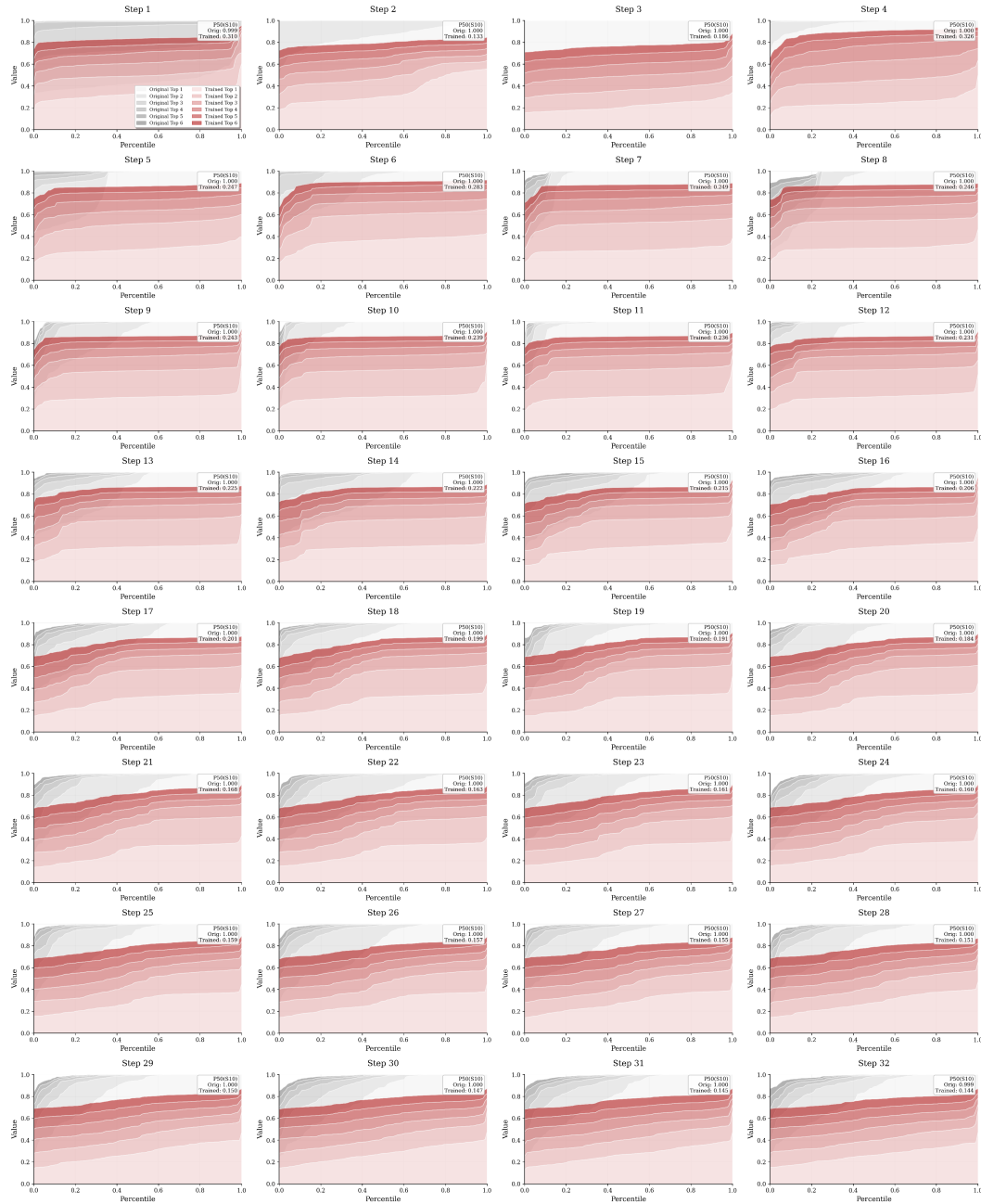


Figure 9: **Extended analysis (32 steps)**. Same construction as Fig. 4, now for steps 1–32. Persistent separation among successive Top- k bands and consistently lower $P_{50}(S_{10})$ values indicate that the trained latents maintain broad, plausible reasoning branches across the entire sequence, despite compression.

F TRAINING TEMPLATE

We present an example in Figure F to illustrate how agents explore and solve tasks in Alfworld. After perceiving the environment, the agent executes an action, receives feedback from the environment, and then proceeds to the next step until the goal is accomplished. Figure F shows an example of how training data is structured for the actor agent. We append either the latent communication or the natural-language plan after the instruction to facilitate inter-agent communication.



Agent

Thought: I'm back at the toilet paper hanger with the roll in hand. It's time to put the toilet paper on the hanger.

Action: put toiletpaper 1 in/on toiletpaperhanger 1

Training Template for Actor Agent

<im_start>system

You are a helpful assistant. <im_end>

<im_start>user

Interact with a household to solve a task. Imagine you are an intelligent agent in a household environment and your target is to perform actions to complete the task goal. At the beginning of your interactions, you will be given a detailed description of the current environment and your goal to accomplish.

For each of your turns, you will be given the observation of the last turn. You should first think about the current condition and plan for your future actions, and then output your action in this turn. Your output must strictly follow this format: "Thought: your thoughts.

Action: your next action".

The available actions are:

1. go to recep
2. task obj from recep
3. put obj in/on recep
4. open recep
5. close recep
6. toggle obj recep
7. clean obj with recep
8. heat obj with recep
9. cool obj with recep

where obj and recep correspond to objects and receptacles.

After your each turn, the environment will give you immediate feedback based on which you plan your next few steps. if the environment output "Nothing happened", that means the previous action is invalid and you should try more options.

Your response should use the following format:

Thought: <your thoughts>

Action: <your next action>

You are in the middle of a room. Looking quickly around you, you see a armchair 2, a armchair 1, a coffeetable 2, a coffeetable 1, a diningtable 1, a garbagecan 1, a sidetable 2, a sidetable 1, and a sofa 1.

Your task is to: find two newspaper and put them in armchair.

Now, you are given a step-by-step plan to complete this task as follow:

<bop>

Insert a latent communication or textual plan for inter-agent communication.

<eop>

<im_end>

<im_start>assistant

Thought: To complete the task, I need to locate two newspapers and place them in an armchair. I should start by searching the nearby furniture for any newspapers.

Action: go to sofa 1 <im_end>

<im_start>user

Observation: On the sofa 1, you see a box 3, a box 2, a newspaper 2, and a pillow 1. <im_end>

<im_start>assistant

Thought: I've found one newspaper on sofa 1. I should pick it up to place it in the armchair later.

Action: take newspaper 2 from sofa 1 <im_end>

<im_start>user

Observation: You pick up the newspaper 2 from the sofa 1. <im_end>

<im_start>assistant
Thought: With newspaper 2 in hand, I need to find the second newspaper. The dining table is another common place where newspapers might be found.
Action: go to dining table 1 <im_end>
<im_start>user
Observation: On the dining table 1, you see a box 1, a credit card 2, a credit card 1, a laptop 1, a newspaper 1, a plate 3, a plate 1, a remote control 1, a statue 3, a statue 1, a tissue box 3, and a tissue box 1. <im_end>
<im_start>assistant
There's the second newspaper on the dining table. I should take it so I can place both newspapers in the armchair as instructed.
Action: take newspaper 1 from dining table 1 <im_end>
<im_start>user
Observation: You pick up the newspaper 1 from the dining table 1. <im_end>
<im_start>assistant
Thought: With both newspapers now in my possession, I need to find an armchair to place them in.
Action: go to armchair 1 <im_end>
<im_start>user
Observation: On the armchair 1, you see a keychain 1. <im_end>
<im_start>assistant
Thought: The armchair has a keychain on it, but there's enough space for the newspapers. I'll place the first newspaper here.
Action: put newspaper 2 in/on armchair 1 <im_end>
<im_start>user
Observation: You put the newspaper 2 in/on the armchair 1. <im_end>
<im_start>assistant
Thought: With the first newspaper placed, I need to put the second newspaper in the armchair to complete the task.
Action: put newspaper 1 in/on armchair 1 <im_end>